



Published in final edited form as:

*Cell*. 2010 September 3; 142(5): 699–713. doi:10.1016/j.cell.2010.07.044.

## Anti-CD47 antibody synergizes with rituximab to promote phagocytosis and eradicate non-Hodgkin lymphoma

Mark P. Chao<sup>1,10</sup>, Ash A. Alizadeh<sup>1,2,3,10</sup>, Chad Tang<sup>1</sup>, June H. Myklebust<sup>3,9</sup>, Bindu Varghese<sup>3</sup>, Saar Gill<sup>5</sup>, Max Jan<sup>1</sup>, Adriel C. Cha<sup>1</sup>, Charles K. Chan<sup>1</sup>, Brent T. Tan<sup>4</sup>, Christopher Y. Park<sup>1,4</sup>, Feifei Zhao<sup>1</sup>, Holbrook E. Kohrt<sup>2,3</sup>, Raquel Malumbres<sup>6</sup>, Javier Briones<sup>7</sup>, Randy D. Gascoyne<sup>8</sup>, Izidore S. Lossos<sup>6</sup>, Ronald Levy<sup>3</sup>, Irving L. Weissman<sup>1,4,10</sup>, and Ravindra Majeti<sup>1,2,10</sup>

<sup>1</sup>Institute for Stem Cell Biology and Regenerative Medicine, Stanford Cancer Center, and Ludwig Center at Stanford, Stanford University, Palo Alto, CA 94304, USA

<sup>2</sup>Department of Internal Medicine, Division of Hematology, Stanford University, Palo Alto, CA 94304, USA

<sup>3</sup>Division of Oncology, Stanford University, Palo Alto, CA 94304, USA

<sup>4</sup>Department of Pathology, Stanford University, Palo Alto, CA 94304, USA

<sup>5</sup>Division of Blood and Bone Marrow Transplantation, Stanford University, Palo Alto, CA 94304, USA

<sup>6</sup>Department of Medicine, Division of Hematology-Oncology, University of Miami Miller School of Medicine, Miami, FL 33136, USA

<sup>7</sup>Department of Hematology, Autonomous University of Barcelona, Barcelona, Spain

<sup>8</sup>Department of Pathology, British Columbia Cancer Agency, Vancouver, Canada

<sup>9</sup>Department of Immunology, Institute for Cancer Research, Oslo University Hospital/Centre for Cancer Biomedicine, University of Oslo

### Summary

Monoclonal antibodies are standard therapeutics for several cancers including the anti-CD20 antibody rituximab for B cell non-Hodgkin lymphoma (NHL). Rituximab and other antibodies are not curative, and must be combined with cytotoxic chemotherapy for clinical benefit. Here we report the eradication of human NHL solely with a monoclonal antibody therapy combining rituximab with a blocking anti-CD47 antibody. We identified increased expression of CD47 on human NHL cells, and determined that higher *CD47* expression independently predicted adverse clinical outcomes in multiple NHL subtypes. Blocking anti-CD47 antibodies preferentially enabled phagocytosis of NHL cells and synergized with rituximab. Treatment of human NHL-engrafted mice with anti-CD47 antibody reduced lymphoma burden and improved survival, while combination treatment with rituximab led to elimination of lymphoma and cure. These antibodies synergized through a mechanism combining Fc receptor (FcR)-dependent and FcR-independent stimulation of phagocytosis that might be applicable to many other cancers.

Correspondence should be addressed to: Mark Chao, Stanford Institute for Stem Cell Biology and Regenerative Medicine, 1050 Arastradero Road, Building A, Palo Alto, CA 94304, mpchao@stanford.edu.

<sup>10</sup>These authors contributed equally to this work

**Publisher's Disclaimer:** This is a PDF file of an unedited manuscript that has been accepted for publication. As a service to our customers we are providing this early version of the manuscript. The manuscript will undergo copyediting, typesetting, and review of the resulting proof before it is published in its final citable form. Please note that during the production process errors may be discovered which could affect the content, and all legal disclaimers that apply to the journal pertain.

## Introduction

Emerging evidence has demonstrated that monoclonal antibodies (mAbs) either alone or in combination are an effective modality for cancer treatment (Adams and Weiner, 2005). Although therapies combining a mAb with chemotherapeutic agents are effective in several human cancers, antibodies alone are not curative. Antibodies effective against cancer are believed to function by several mechanisms including: antibody-dependent cellular cytotoxicity (ADCC), stimulation of complement-dependent cytotoxicity (CDC), inhibition of signal transduction, or direct induction of apoptosis (Cheson and Leonard, 2008).

Non-Hodgkin lymphoma (NHL) is the fifth most common cancer in the United States consisting of indolent and aggressive subtypes with a five-year overall survival ranging from 25-75% (1993). The anti-CD20 antibody, rituximab (Rituxan), is a standard therapy for many CD20-positive B cell lymphomas, and significantly improves long-term survival in combination with conventional chemotherapy (Cheson and Leonard, 2008). As a single agent or in combination with chemotherapy, rituximab is not curative in the majority of B cell NHL patients and rituximab resistance has been observed (reviewed in (Cheson and Leonard, 2008). Multiple lines of evidence indicate that rituximab acts at least in part by engaging Fc receptors (FcRs) on immune effector cells, such as NK cells and macrophages, and stimulating effector functions such as ADCC (Glennie et al., 2007; Nimmerjahn and Ravetch, 2007). Although resistance has been reported to occur through several mechanisms (Cartron et al., 2004), there has been limited development of agents that can overcome this resistance.

Immune effector cells, including NK cells and phagocytes, are critical to the efficacy of many anti-cancer antibodies. Phagocytic cells, including macrophages and dendritic cells, express signal regulatory protein alpha (SIRP $\alpha$ ), which binds CD47, a widely expressed transmembrane protein (Brown and Frazier, 2001). CD47-mediated activation of SIRP $\alpha$  initiates a signal transduction cascade resulting in inhibition of phagocytosis (reviewed in (Jaiswal et al.)). In identifying a role for CD47 in cancer pathogenesis, we previously demonstrated that forced expression of mouse CD47 on a human leukemia cell line facilitated tumor engraftment in immunodeficient mice through the evasion of phagocytosis (Jaiswal et al., 2009). We further demonstrated that this mechanism could be targeted therapeutically in human acute myeloid leukemia (AML) with a blocking anti-CD47 antibody that enabled phagocytosis and eliminated AML stem cells (Majeti et al., 2009). Based on this antibody mechanism, we hypothesized that the combination of a blocking anti-CD47 antibody with a second FcR-activating antibody would both prevent an inhibitory signal and deliver a positive stimulus resulting in the synergistic phagocytosis and elimination of target cells. Here, we tested this antibody synergy hypothesis by investigating the combination of a blocking anti-CD47 mAb with rituximab against human NHL.

## Results

### CD47 Expression is Increased on NHL Cells Compared to Normal B Cells

We examined CD47 protein expression on primary human NHL samples and normal B cells by flow cytometry. Compared to both normal peripheral blood and germinal center B cells, CD47 was more highly expressed on a large subset of primary patient samples from multiple B cell NHL subtypes (Figure 1A and S1A), including Diffuse Large B Cell Lymphoma (DLBCL), B cell Chronic Lymphocytic Leukemia (B-CLL), Mantle Cell Lymphoma (MCL), Follicular Lymphoma (FL), Marginal Zone Lymphoma (MZL) and pre-B acute lymphoblastic leukemia (pre-B ALL). Across NHL subtypes, we found differing levels of CD47 expression that also varied within each NHL subtype (Figure 1B).

## Increased CD47 Expression Correlates with a Worse Clinical Prognosis and Adverse Molecular Features in Multiple NHL Subtypes

Having previously shown a correlation between *CD47* mRNA and protein expression (Majeti et al., 2009), we assessed *CD47* mRNA expression across NHL subtypes for associations with morphologic and molecular subgroups using gene expression data from previously described patient cohorts (Table S1) and investigated the prognostic implications of increased *CD47* expression in disease outcome. Higher *CD47* expression was associated with adverse prognosis in DLBCL, B-CLL, and MCL (Figure 1C-E). In patients with DLBCL, whether treated with or without rituximab-based combination chemotherapy (Figures 1C and S1B), higher *CD47* expression was significantly associated with risk of death. This increased risk was largely due to disease progression (Figure S1C), a finding validated in an independent cohort of patients using quantitative RT-PCR on fixed archival specimens (Figure S1D).

We next investigated whether increased *CD47* expression was associated with known adverse molecular features in NHL. In DLBCL, prior studies have identified two distinct subgroups based on the presumed cell of origin of tumors: normal germinal center B cells (GCB-like), which is associated with a favorable clinical outcome, or activated blood memory B cells (ABC-like), which is associated with a poor clinical outcome (Alizadeh et al., 2000; Rosenwald et al., 2002; Shipp et al., 2002). *CD47* expression was significantly higher in ABC-like DLBCL (Figures 1F and S1E). *CD47* expression was not found to have independent prognostic value within GCB and ABC subtypes, suggesting a strong association with the cell-of-origin classification of DLBCL. Higher *CD47* expression was also associated with unmutated immunoglobulin heavy chain variable regions (IgVH) in CLL (Figures 1G and S1F) and significantly correlated with the proliferative index in MCL (Figure 1H), both known adverse prognostic factors (Katzenberger et al., 2006; Oscier et al., 2002; Rosenwald et al., 2003). In multivariate analyses, *CD47* expression remained prognostic of disease progression independent from the international prognostic index in DLBCL (1993), and two major prognostic factors in CLL: IgVH mutation status and ZAP-70 status (Figure S1G). Within the small MCL cohort, a multivariate model did not find independent prognostic value for *CD47* when considering the proliferation index (data not shown).

## Blocking Anti-CD47 Antibodies Enable Phagocytosis of NHL Cells by Macrophages and Synergize with Rituximab *in Vitro*

We first tested the ability of anti-human CD47 antibodies to enable phagocytosis of human NHL cell lines, primary NHL cells, and normal peripheral blood (NPB) cells by human macrophages *in vitro*. Incubation of NHL cells in the presence of IgG1 isotype control or anti-CD45 IgG1 antibody did not result in significant phagocytosis; however, two different blocking anti-CD47 antibodies (B6H12.2 and BRIC126) enabled phagocytosis of NHL cells, but not NPB cells (Figure 2A,B).

Next, we repeated the *in vitro* phagocytosis assays with mouse macrophages. Incubation of NHL cells in the presence of IgG1 isotype control or anti-CD45 IgG1 antibody did not result in significant phagocytosis; however, phagocytosis of NHL cells was observed with blocking antibodies to CD47 (B6H12.2 and BRIC126), while no phagocytosis was observed with a non-blocking antibody (2D3) (Figure 2B). Disruption of the CD47-SIRP $\alpha$  interaction with an anti-mouse SIRP $\alpha$  antibody also resulted in significant phagocytosis (Figure 2B).

Given variable expression of CD47 on primary NHL, we investigated whether CD47 expression levels correlated with the degree of anti-CD47 antibody-mediated phagocytosis by two independent methods. First, lentiviral shRNA vectors were used to knockdown

expression of CD47 in Raji cells. Several clones were generated with a range of CD47-knockdown (Figure S2A,B). Those clones with a greater than 50% reduction in CD47 expression (shCD47-1 and shCD47-2) demonstrated a significant reduction in anti-CD47 antibody-mediated phagocytosis (Figure S3C). In the second approach, a statistical analysis demonstrated a positive correlation between CD47 expression and degree of anti-CD47 antibody-mediated phagocytosis with both mouse and human macrophages effector cells (Figure S2D).

It has been reported that immobilized or cross-linked antibodies against CD47 induce apoptosis of primary human B-CLL cells, as well as several malignant lymphoid cell lines (Kikuchi et al., 2005; Kikuchi et al., 2004; Mateo et al., 1999; Uno et al., 2007). Therefore, anti-CD47 antibodies might be predicted to directly induce apoptosis of NHL cells that are then recognized by macrophages and phagocytosed. Contrary to this prediction, when NHL cells were incubated with anti-CD47 antibody in the absence of macrophages, no induction of apoptosis was observed when cells were incubated in suspension for either two hours (Figure 2B, right) or eight hours (Figure S2E,F). Incubation of NHL cells with immobilized anti-CD47 antibody resulted in increased apoptosis compared to controls (Figure S2G,H), consistent with prior reports (Mateo et al., 1999). Since phagocytosis of NHL cells occurs in the presence of soluble anti-CD47 mAbs, it is unlikely that these mAbs induce apoptosis of NHL cells that are then secondarily phagocytosed.

Next, we tested the ability of a blocking anti-CD47 mAb to synergize with rituximab in the phagocytosis of NHL cells. We examined CD20 expression on NHL cells and found no difference between normal B cells and NHL cells (Figure S2I,J). Incubation of NHL cells with rituximab in the presence of mouse or human macrophages resulted in significant phagocytosis (Figure 2D,E). We then tested the synergy hypothesis by isobologram analysis (Chou, 2008; Tallarida, 2006). Using Raji, SUDHL4, and NHL17 cells, which express varying levels of both CD47 and CD20 (Figure S2K), anti-CD47 antibody synergized with rituximab or anti-human CD20 (mouse IgG2a) antibody, as indicated by combination indices less than 1 (Figure 2C). In a second approach, *in vitro* phagocytosis assays were conducted with primary NHL cells incubated with either anti-CD47 antibody or rituximab alone, or both in combination at half of the single agent dose. NHL cells exhibited a significant increase in phagocytosis when incubated with the combination compared to either antibody alone when using mouse (Figure 2D) or human (Figure 2E) macrophage effectors. No phagocytosis of NPB cells was observed with either antibody alone or in combination with human macrophages (Figure 2E).

### Ex Vivo Coating of NHL Cells with an Anti-CD47 Antibody Inhibits Tumor Engraftment

Next, the ability of blocking anti-CD47 antibody to eliminate NHL *in vivo* either alone or in combination with rituximab was explored by two separate treatment strategies. First, the effect of *ex vivo* anti-CD47 antibody coating on the engraftment of human NHL cells was tested. Luciferase-expressing Raji and SUDHL4 cell lines were pre-coated *ex vivo* with anti-CD47, IgG1 isotype control, or anti-CD45 antibody and transplanted intravenously into SCID mice. Coating with anti-CD47 antibody prevented engraftment of both cell lines (Figure 3A-F). Coating of Raji cells with rituximab also inhibited engraftment when transplanted into SCID mice (Figure S3). In addition to these cell lines, we identified a primary NHL patient specimen that engrafted in NSG mice in the bone marrow upon intravenous transplantation (Figure S5A,B). As with the cell lines, *ex vivo* coating of these primary cells with anti-CD47 antibody, but not controls (Figure 3G), resulted in complete inhibition of bone marrow engraftment (Figure 3H).

## Combination Therapy with Anti-CD47 Antibody and Rituximab Eliminates Lymphoma in Both Disseminated and Localized Human NHL Xenotransplant Models

In the second treatment strategy, mice were first engrafted with NHL and then administered single or combination antibody therapy. To best model NHL, we established disseminated and localized xenotransplantation models in NSG mice that are deficient in T, B, and NK cells (Shultz et al., 2005), but retain phagocyte effector cells. In the disseminated model, luciferase-expressing Raji cells were transplanted intravenously into adult NSG mice. Two weeks later, these mice were administered daily injections of either control mouse IgG, anti-CD47 antibody, rituximab, or anti-CD47 antibody and rituximab. Anti-CD47 antibody treatment decreased the lymphoma burden in these mice (Figure 4A,B), and significantly prolonged survival compared to control IgG, although all mice eventually died (Figure 4C and Table S2). Similar results were seen with rituximab, and were not statistically different compared to anti-CD47 antibody (Figure 4A-C and Table S2). In contrast, combination therapy with anti-CD47 antibody and rituximab eliminated lymphoma in 60% of mice as indicated by long-term survival (Figure 4C) and the absence of luciferase-positive lymphoma (data not shown) more than four months after the end of treatment. In humans, rituximab efficacy is thought to be primarily mediated by both macrophages and NK cells (Nimmerjahn and Ravetch, 2007; Taylor and Lindorfer, 2008). Given that NSG mice lack NK cells, we conducted a similar experiment in NK cell-containing SCID mice, and observed similar therapeutic responses as in NSG mice (Figure S4A,B).

In the localized NHL model, luciferase-expressing Raji cells were transplanted subcutaneously in the right flank of NSG mice. Once tumors were palpable (approximately 2 weeks), mice were treated with antibody therapy. Mice treated with anti-CD47 antibody or rituximab demonstrated a decreased rate of lymphoma growth compared to control IgG-treated mice as measured by both luciferase signal and tumor volume (Figure 4D-F), however like controls, eventually had to be sacrificed due to enlarged tumor growth. In contrast, mice treated with the combination of anti-CD47 antibody and rituximab demonstrated complete elimination of lymphoma, with 86% of treated mice having no measurable mass or luciferase-positive lymphoma 4 weeks after the end of therapy (Figures 4D-F and S4C-E). Moreover, all showed no evidence of tumor growth, remained relapse free, and were alive at over 197 days after tumor engraftment. Out of six mice achieving a complete remission, five remained relapse free while one mouse died of non-tumor related causes (Figure 4E). For both disseminated and localized xenograft models, expression of CD47 and CD20 in transplanted Raji cells did not differ from Raji cells in culture (Figure S4F).

## Combination Therapy with Anti-CD47 Antibody and Rituximab Eliminates Lymphoma in Primary Human NHL Xenotransplant Mouse Models

NHL cell lines have been valuable for the evaluation of therapeutics, but they may not accurately recapitulate the heterogeneity of the primary disease. We report here two new mouse xenograft models for NHL in which intravenous transplantation of cells from a DLBCL patient (NHL7/SUNHL7) and a FL patient (NHL31/SUNHL31) give rise to robust lymphoma engraftment in the bone marrow and/or peripheral blood (Figures S1A and S5A). Primary DLBCL cells were transplanted into mice, which two weeks later were treated with daily injections of antibodies for 14 days. Treatment with anti-CD47 antibody either alone or in combination with rituximab eliminated human lymphoma in the bone marrow, while treatment with rituximab resulted in a reduction of disease in 60% of mice (Figure 5A,B). Mouse hematopoietic cells were unaffected by antibody therapy (Figure S5E). Treatment was then discontinued, and all mice were monitored for survival. Mice treated with either anti-CD47 antibody or rituximab alone had a significantly longer survival compared to mice treated with control IgG, but all eventually died secondary to disease due to widespread

organ dissemination on autopsy (Figure 5C, data not shown). Most significantly, 8 out of 9 mice (89%) administered combination antibody treatment were cured of lymphoma, as indicated by long-term disease-free survival more than 4 months after the end of treatment (Figure 5C and Table S3) with no detectable lymphoma in the bone marrow (data not shown). In a second primary model, FL cells were transplanted intravenously in a similar manner. CD20+CD10+ lymphoma engraftment in the peripheral blood and bone marrow was detected after 8 weeks. At this time, mice were treated with a single intraperitoneal injection of either control IgG, anti-CD47 antibody, rituximab, or the combination and then followed for disease progression. A single dose of anti-CD47 antibody alone or in combination with rituximab eliminated lymphoma both in the peripheral blood (Figure 5D) and bone marrow (Figure 5E). In contrast, a single dose of rituximab enabled a partial reduction in tumor burden that rebounded back to baseline levels in the peripheral blood with no tumor reduction observed in the bone marrow. The difference in anti-CD47 antibody clearance of lymphoma as a single dose in FL-engrafted mice (Figure 5D,E) compared to multiple dose therapy in mice engrafted with DLBCL (Figure 5B) or Raji (Figure 4) may be due to cell-intrinsic differences in antibody sensitivity between different NHL subtypes or due to different anti-CD47 antibody potencies in distinct tissue compartments (peripheral blood vs. BM vs. soft tissue compartments).

To assess the ability of these two primary NHL xenotransplant models to model the disease, we compared histological sections of the primary NHL specimen and the transplanted tumor. Similar DLBCL and FL morphology was observed for NHL7 and NHL31, respectively (Figure S5B). We next determined whether the percentage of macrophages infiltrating the tumor differed between the primary patient and the xenografted tumor. For NHL31, the percentage of infiltrating human macrophages (CD68+) in the primary lymph node was similar to the percentage of infiltrating mouse macrophages (F4/80+) in bone marrow of transplanted mice (Figure S5C). Analyzing infiltrating macrophage frequency by flow cytometry, no difference was observed between the primary specimen and xenograft for either NHL7 or NHL31 (Figure S5D).

### **Synergy Between Anti-CD47 Antibody and Rituximab Does Not Occur Through NK Cells or Complement**

Rituximab can eliminate malignant cells via apoptosis, NK cell-mediated ADCC, and CDC (reviewed in (Smith, 2003)). However, it is not known whether anti-CD47 antibody also enables ADCC or CDC in addition to phagocytosis. Therefore, we investigated whether anti-CD47 antibody alone could induce anti-tumor effects by macrophage-independent mechanisms, and whether synergy with rituximab could occur through these modalities. First, to investigate possible synergy in direct apoptosis, NHL cells were incubated with either anti-CD47 antibody/rituximab alone or in combination without macrophages, and cell death was measured. No synergistic apoptosis was observed when NHL cells were incubated with soluble (Figures 6A and S6A) or immobilized (Figure S6B,C) antibodies. Furthermore, cross-linking of soluble anti-CD47 antibody alone or in combination with rituximab by macrophages did not induce increased apoptosis of non-phagocytosed NHL cells compared to IgG1 isotype control, while rituximab induced a slight increase in apoptosis (Figure S6D). No synergistic apoptosis was observed in this context (Figure S6D). The small increase in apoptosis upon antibody treatment was not FcR-dependent given that results were similar with macrophages lacking the Fc $\gamma$  subunit (Takai et al., 1994) (Figure S6D). Second, we investigated whether NK cells could mediate tumor elimination by anti-CD47 antibody alone or in synergy with rituximab. A prior report observed increased NK-cell cytotoxicity of cancer cell lines with an anti-CD47 antibody *in vitro*, though the mechanism of targeting was not elucidated (Kim et al., 2008). We first determined whether human or mouse NK cells expressed SIRP $\alpha$ , and found that both human NK cells, CD3-CD56+CD7+ (Milush et

al., 2009), as well as mouse NK cells, CD3-DX5+, expressed minimal to no SIRP $\alpha$  (Figure 6B). Next, the ability of anti-CD47 antibody to induce NK cell-mediated ADCC through FcRs or by CD47-SIRP $\alpha$  blockade was investigated. Utilizing human NK cells as effectors, anti-CD47 antibody did not induce increased ADCC of Raji or SUDHL4 cells compared to IgG1 isotype control (Figure 6C). While rituximab did enable ADCC of these two NHL cell lines, no synergistic effect between anti-CD47 antibody and rituximab was observed ( $p=0.77$ , Figure 6C). Since anti-CD47 antibody (B6H12.2) is a mouse IgG1 isotype, we repeated these assays with mouse NK cells. Anti-CD47 antibody caused increased ADCC of these two NHL cell lines compared to isotype control, while rituximab induced ADCC to a lesser degree (Figure 6D). To test whether anti-CD47 antibody-mediated ADCC was Fc-dependent, we generated a F(ab')<sub>2</sub> fragment of the anti-CD47 antibody (Figure S7B-I). The F(ab')<sub>2</sub> fragment did not enable ADCC, indicating that the increased ADCC was likely mediated through FcRs (Figure 6D). The combination of anti-CD47 antibody or F(ab')<sub>2</sub> fragment with rituximab did not induce a statistically significant increase in ADCC compared to single agent therapy, indicating no synergistic effect. Third, we investigated the role of complement in anti-CD47 antibody-mediated cytotoxicity. Using either human (Figure 6E) or mouse (Figure 6F) complement, anti-CD47 antibody did not induce CDC of either an NHL cell line or a primary NHL sample, while rituximab did induce significant CDC against both of these samples. Moreover, the combination of anti-CD47 antibody and rituximab did not induce increased CDC compared to rituximab alone. Fourth, we investigated the relative contribution of major components of macrophages, NK cells, and complement in mediating the therapeutic effects of anti-CD47 antibody and rituximab *in vivo*. Luciferase-labeled Raji cells were engrafted intravenously into SCID mice, which have functional macrophages, NK cells, and complement. Mice were then separated into cohorts receiving selective depletion of either macrophages by clodronate, NK cells by anti-asialoGM1 antibody, complement by cobra venom factor, or a vehicle control. These cohorts were then treated with combination anti-CD47 antibody and rituximab therapy for 3 days, and tumor burden was measured by bioluminescent imaging pre- and post-treatment. Compared to vehicle control, NK cell and complement depletion had no effect on tumor elimination by combination antibody therapy (Figure S6E). In contrast, macrophage depletion significantly abrogated the therapeutic effect, indicating that macrophages, and not NK cells or complement, are required for combination anti-CD47 antibody and rituximab-mediated elimination of NHL *in vivo*.

### Anti-CD47 Antibody Synergizes with Rituximab Through FcR-Independent and FcR-Dependent Mechanisms

We hypothesize that the observed synergy between an anti-CD47 antibody and rituximab occurs through the combination of two separate mechanisms for stimulating phagocytosis: (1) FcR-independent through blockade of an inhibitory phagocytic signal by anti-CD47 antibody, and (2) FcR-dependent through delivery of a positive phagocytic signal by rituximab. We utilized four independent methods to investigate this hypothesis. First, synergistic phagocytosis was observed with the combination of anti-SIRP $\alpha$  antibody and rituximab by isobologram analysis (Figure 7A), and with a large panel of primary NHL samples (Figure 7B). Second, mouse macrophages lacking the Fc $\gamma$  receptor, thereby incapable of enabling FcR-dependent phagocytosis (Takai et al., 1994), but still expressing SIRP $\alpha$  (Figure S7A), were utilized as effector cells for phagocytosis of NHL cells incubated with either anti-CD47 antibody, anti-SIRP $\alpha$  antibody, rituximab, or anti-CD47/anti-SIRP $\alpha$  antibody in combination with rituximab. As predicted, anti-CD47 antibody and anti-SIRP $\alpha$  antibody, but not rituximab, enabled phagocytosis of NHL cells, without evidence of synergistic phagocytosis (Figure 7C).

Third, F(ab')<sub>2</sub> fragments of both anti-CD47 antibody and rituximab were generated (Figure S7B-I) and utilized in phagocytosis assays with NHL cells and wild type macrophages. Anti-CD47 F(ab')<sub>2</sub> antibody synergized with rituximab as demonstrated by isobologram analysis (Figure 7D). Additionally, anti-CD47 F(ab')<sub>2</sub>, but not rituximab F(ab')<sub>2</sub>, enabled phagocytosis of NHL cells (Figure 7E). Consistent with the proposed mechanism, synergistic phagocytosis was observed with the combination of either full length anti-CD47 or anti-CD47 F(ab')<sub>2</sub> with full length rituximab, but not with any combination involving rituximab F(ab')<sub>2</sub> (Figure 7E).

Fourth, synergistic phagocytosis was investigated *in vivo* using GFP+ Raji cells engrafted in NSG mice. As single agents, anti-CD47 antibody and rituximab enabled phagocytosis of Raji cells engrafted in the liver as evidenced by an increased percentage of mouse macrophages containing phagocytosed GFP+Raji cells (Figure 7F). Most significantly, combination anti-CD47 antibody and rituximab treatment enabled significantly increased phagocytosis compared to either single agent demonstrating that synergistic phagocytosis occurred *in vivo* (Figure 7F).

## Discussion

In this report, we identify a distinct mechanism of synergy between mAbs in cancer therapy leading to cures in the absence of chemotherapy. Specifically, we utilized a blocking anti-CD47 antibody in combination with the anti-CD20 antibody rituximab to eradicate human NHL through a mechanism of synergy involving FcR-independent enabling of phagocytosis by anti-CD47 antibody and FcR-dependent stimulation of phagocytosis by rituximab. In addition, the identification of *CD47* expression as a prognostic factor could be incorporated into standard clinical prognostic considerations across multiple subtypes of NHL, and may be useful in risk-adapted therapy decision-making.

While it is thought that many therapeutic mAbs for human malignancies, including rituximab, function primarily through NK cell-mediated ADCC, several lines of evidence indicate that the therapeutic effect of anti-CD47 antibody alone or in combination with rituximab is mediated primarily through macrophage phagocytosis. First, synergistic macrophages phagocytosis was observed with combination anti-CD47 antibody and rituximab *in vitro*, while no synergy was observed for direct apoptosis, ADCC, or CDC (Figures 2C-E, S6, 6A, and 6C-F). Second, phagocytosis of NHL cells *in vivo* was observed with either anti-CD47 antibody or rituximab alone, and most importantly, significantly increased with combination therapy (Figure 7F). Third, the therapeutic effect of combination antibody treatment was similar in an NHL xenotransplant model using complement and NK cell-deficient NSG mice (Figure 4C) as in complement and NK cell-competent SCID mice (Figure S4A,B), suggesting that macrophages alone are sufficient to mediate the therapeutic effect. Fourth, depletion of macrophages, but not complement or NK cells abrogated the synergistic effect of anti-CD47 antibody in combination with rituximab (Figure S6E). These studies highlight the importance of macrophages as effectors of anti-CD47 antibody therapy in human NHL.

This study describes a mechanism of antibody synergy in the elimination of NHL in the absence of chemotherapy. Combination antibody therapies for NHL have previously been investigated, mostly in combination with rituximab, with some progressing to clinical trials. These include a humanized antibody targeting the B cell antigen CD22 (epratuzumab) and galiximab, a chimeric antibody targeting the co-stimulatory ligand CD80. Phase I/II studies with either epratuzumab or galiximab in combination with rituximab demonstrate relative safety and clinical responses equal to or greater than single agent therapy alone (Leonard et al., 2005; Leonard et al., 2007; Leonard et al., 2008). Based on these results, phase III trials



are underway. Antibody combinations involving anti-CD20 antibodies and antibodies to pro-apoptotic receptors are also being explored in pre-clinically (Daniel et al., 2007; Maddipatla et al., 2007). These studies highlight the clinical potential of combination antibody approaches in NHL patients.

Combination therapy with two or more mAbs possesses several advantages compared to monotherapies in NHL or other malignancies. First, therapy solely with monoclonal antibodies targeting cancer-specific antigens could result in decreased off-target toxicity compared to current therapeutic regimens that utilize chemotherapy. Second, synergy between two distinct antibody effector mechanisms, FcR-independent and FcR-dependent as shown here, would result in increased therapeutic efficacy. Third, antibody targeting of two distinct cell-surface antigens would be more likely to eliminate cancer cells with pre-existing epitope variants or epitope loss, such as those reported in rituximab-refractory/resistant NHL patients (Foran et al., 2001; Hiraga et al., 2009; Kennedy et al., 2004). Fourth, a bispecific FcR-engaging antibody with one arm binding and blocking CD47 and the other binding to a validated cancer antibody target (CD20) could reduce potential antibody toxicity, while retaining the synergy effect, especially since CD47 is expressed in multiple normal tissue types. Although we demonstrated that an anti-mouse CD47 antibody is relatively non-toxic to wild type mice (Majeti et al., 2009), a clinical anti-human CD47 antibody may have a different human toxicity profile that could be overcome by a bispecific antibody.

In addition to its application in NHL, the reported mechanism of antibody synergy provides proof-of-principle that a blocking mAb directed against CD47 can synergize with an FcR-activating antibody to provide superior therapeutic efficacy. This finding raises the possibility of potential synergy between an anti-CD47 antibody and other clinically approved therapeutic antibodies that may activate FcRs on immune effector cells for the treatment of diverse human malignancies including: trastuzumab (Herceptin) for HER2-positive breast carcinomas, cetuximab (Erbix) for colorectal carcinomas and head and neck squamous cell carcinomas, alemtuzumab (Campath) for CLL and T-cell lymphoma, and others in development (Finn, 2008). To date, we have demonstrated effective anti-CD47 antibody targeting of several human cancers including AML (Majeti et al., 2009), bladder cancer (Chan et al., 2009), and now NHL, leading us to speculate that CD47 targeting will be effective against a wide range of human cancers.

## Experimental Procedures

### Cell lines

A Burkitt's lymphoma cell line (Raji) and a DLBCL cell line (SUDHL4) were obtained from the American Type Culture Collection or generated in the lab. The NHL17\* cell line was generated from a patient with DLBCL by culturing bulk cells *in vitro* with IMDM supplemented with 10% human AB serum for 1.5 months.

### Human Samples

Normal human peripheral blood and human NHL samples were obtained the Stanford University Medical Center, Stanford, CA with informed consent, according to an IRB-approved protocol (Stanford IRB# 13500) or with informed consent from the Norwegian Radium Hospital, Oslo, Norway according to a Regional Ethic Committee (REK)-approved protocol (REK# 2.2007.2949). Normal tonsils for germinal center B cell analysis were obtained from discarded tonsillectomy specimens from consented pediatric patients at Stanford University Medical Center according to an IRB-approved protocol (Stanford IRB# 13500).

## Flow Cytometry Analysis

For analysis of normal peripheral blood cells, germinal center B cells, and primary NHL cells, the following antibodies were used: CD19, CD20, CD3, CD10, CD45, CD5, CD38 (Invitrogen, Carlsbad, CA and BD Biosciences, San Jose, CA). Analysis of CD47 expression was performed with an anti-human CD47 FITC antibody (clone B6H12.2, BD Biosciences). Cell staining and flow cytometry analysis was performed as previously described (Majeti et al., 2009).

## Evaluation of Prognostic Value of CD47 in NHL

Gene expression and clinical data were analyzed for 8 previously described cohorts of adult NHL patients, including 4 studies of patients with DLBCL, 3 with B-CLL, and 1 with MCL (detailed in Table S1). The clinical end points analyzed included overall (OS), progression free (PFS), and event-free survival (EFS), with events defined as the interval between study enrollment and need for therapy or death from any cause, with data censored for patients who did not have an event at the last follow-up visit. See supplemental section for a detailed description of the analyses.

## Therapeutic Antibodies

Rituximab (anti-CD20, human IgG1) was obtained from the Stanford University Medical Center, mouse anti-human CD20, IgG2a from Beckman Coulter (Miami, FL), and anti-CD47 antibody BRIC126, IgG2b from AbD Serotec (Raleigh, NC). Other anti-CD47 antibodies were used as in (Majeti et al., 2009). All *in vivo* antibody experiments were performed using the anti-CD47 B6H12.2 antibody.

## *In Vitro* Isobologram Studies

*In vitro* phagocytosis assays were conducted with NHL cells incubated with anti-CD47 antibody (B6H12.2), anti-CD20 IgG2a, or rituximab either alone or in combination at concentrations from 1 µg/ml to 10 µg/ml. The concentration of each antibody required to produce a defined single-agent effect (phagocytic index) was determined for each cell type. Concentrations of the two antibodies combined to achieve this same phagocytic index were then plotted on an isobologram and the combination index (CI) determined. The CI was calculated from the formula  $CI = (d1/D1) + (d2/D2)$ , whereby  $d1$ =dose of drug 1 in combination to achieve the phagocytic index,  $d2$ =dose of drug 2 in combination to achieve the phagocytic index,  $D1$ =dose of drug 1 alone to achieve the phagocytic index,  $D2$ =dose of drug 2 alone to achieve the phagocytic index. A CI of less than, equal to, and greater than 1 indicates synergy, additivity, and antagonism, respectively.

## Annexin V Apoptosis Assays

Assays were performed as previously described (Majeti et al., 2009).

## Preparation of human and mouse immune effector cells, immune effector cytotoxicity assays, and *In vivo* depletion of immune effector cells

See supplementary section.

## Preparation of F(ab')<sub>2</sub> fragments

See supplementary section.

## Generation of Luciferase-Positive Cell Lines and Luciferase Imaging Analysis

See supplementary section.

### **In Vivo Pre-Coating Engraftment Assay**

Assays were performed as previously described (Majeti et al., 2009). Pre-coated cells were transplanted intravenously into SCID mice or sublethally-irradiated (200 rads) NOD.Cg-*Prkdc<sup>scid</sup>Il2rg<sup>tm1Wjl</sup>/SzJ* (NSG). All experiments involving mice were performed according to Stanford University institutional animal guidelines.

### **In Vivo Antibody Treatment in a Disseminated Lymphoma Xenograft Model**

$1.5 \times 10^6$  luciferase-labeled Raji cells were injected intravenously into the retro-orbital sinus of 6-10 week old SCID or NSG mice. Those mice with luciferase-positive lymphoma were given daily intraperitoneal injections of 200 $\mu$ g mouse IgG control, anti-CD47, rituximab, or 200 $\mu$ g anti-CD47 + 200 $\mu$ g rituximab for three weeks. Antibody treatment was then stopped and mice were followed for survival analysis. A complete remission (CR) was defined as no evidence of lymphoma by bioluminescence at the end of treatment. A relapse was defined as evidence of lymphoma by bioluminescence after the end of treatment in a mouse with a prior CR.

### **In Vivo Antibody Treatment in a Localized Lymphoma Xenograft Model**

$3 \times 10^6$  luciferase-labeled Raji cells were injected subcutaneously into the right flank of 6-10 week old NSG mice. Those mice with luciferase-positive lymphoma were given daily intraperitoneal injections of 400 $\mu$ g mouse IgG control, 400 $\mu$ g anti-CD47, 200 $\mu$ g rituximab, or 400 $\mu$ g anti-CD47 + 200 $\mu$ g rituximab for four weeks. Tumor volume was measured every 3-4 days using the formula (length\*width)/2. Antibody treatment was then stopped and mice were followed for survival analysis.

### **In Vivo Antibody Treatment of Primary NHL Engrafted Mice**

$2 \times 10^6$  NHL cells were transplanted intravenously via retro-orbital plexus into sublethally-irradiated NSG mice. Two to ten weeks later, bone marrow was aspirated from these mice and those mice with evidence of human lymphoma engraftment (hCD45+CD19/CD10+ bone marrow cells) were then treated with the same antibody regimen as in the disseminated lymphoma model. After 14 days, bone marrow cells from these mice were aspirated and antibody treatment was stopped and mice followed for survival analysis. A complete remission (CR) was defined as no evidence of lymphoma in the BM at end of treatment. A relapse was defined as evidence of lymphoma in the BM after end of treatment in a mouse with a prior CR.

### **In vivo phagocytosis**

*In vivo* phagocytosis was performed as previously described (Majeti et al., 2009) analyzing mice transplanted with GFP+Raji cells into adult NSG mice. Mice were given a single dose of antibody and analyzed 4 hours later for *in vivo* phagocytosis.

## **Supplementary Material**

Refer to Web version on PubMed Central for supplementary material.

## **Acknowledgments**

The authors acknowledge Dr. Christopher Contag for providing luciferase constructs, Dr. Robert Negrin for assistance, Dr. Yaso Natkunam for immunohistochemistry, Libuse Jerabek and Theresa Storm for lab management, and Adriane Mosely for animal husbandry. We also acknowledge the patients and surgeons including Drs. Wapnir, Chang, Cheng, Janisiewicz, Koltai, Liebowitz, and Messner for providing research specimens. M.P.C. is supported by the HHMI and the Stanford Cancer Biology Program, A.A.A. by an NIH T32 Ruth L. Kirschstein National Research Service Award (HL007970), R. Malumbres by a fellowship from Fundación Caja Madrid, I.S.L. by NIH

grant CA122105, and R. Majeti by a grant from the AACR. R. Majeti holds a Career Award for Medical Scientists from the Burroughs Wellcome Fund. I.L.W., M.P.C., and R. Majeti have filed U.S. Patent Application Serial No. 12/321,215 entitled "Methods For Manipulating Phagocytosis Mediated by CD47." This research is supported by NIH grant P01CA139490 to I.L.W. and funding from the Smith Family Fund.

M.P.C., A.A.A., I.L.W., and R. Majeti designed the experiments and. M.P.C., A.A.A., I.L.W., and R. Majeti wrote the manuscript. M.P.C., A.A.A., C.Z.T., J.H.M., S.G., M.J., A.C.C., C.C.K., B.T.T., C.Y.P., F.Z., R. Malumbres, and I.S.L. performed the experiments and analyzed data. J.B., R.D.G., and I.S.L. provided patient samples and clinical data. H.E.K. provided reagents. B.V. generated F(ab')<sub>2</sub> fragments of anti-CD47 antibody and rituximab. All authors endorse the full content of this work.

## References

- A predictive model for aggressive non-Hodgkin's lymphoma. The International Non-Hodgkin's Lymphoma Prognostic Factors Project. *N Engl J Med.* 1993; 329:987–994. [PubMed: 8141877]
- Adams GP, Weiner LM. Monoclonal antibody therapy of cancer. *Nat Biotechnol.* 2005; 23:1147–1157. [PubMed: 16151408]
- Alizadeh AA, Eisen MB, Davis RE, Ma C, Lossos IS, Rosenwald A, Boldrick JC, Sabet H, Tran T, Yu X, et al. Distinct types of diffuse large B-cell lymphoma identified by gene expression profiling. *Nature.* 2000; 403:503–511. [PubMed: 10676951]
- Brown EJ, Frazier WA. Integrin-associated protein (CD47) and its ligands. *Trends Cell Biol.* 2001; 11:130–135. [PubMed: 11306274]
- Cartron G, Watier H, Golay J, Solal-Celigny P. From the bench to the bedside: ways to improve rituximab efficacy. *Blood.* 2004; 104:2635–2642. [PubMed: 15226177]
- Chan KS, Espinosa I, Chao M, Wong D, Ailles L, Diehn M, Gill H, Presti J Jr, Chang HY, van de Rijn M, et al. Identification, molecular characterization, clinical prognosis, and therapeutic targeting of human bladder tumor-initiating cells. *Proc Natl Acad Sci U S A.* 2009; 106:14016–14021. [PubMed: 19666525]
- Cheson BD, Leonard JP. Monoclonal antibody therapy for B-cell non-Hodgkin's lymphoma. *N Engl J Med.* 2008; 359:613–626. [PubMed: 18687642]
- Chou TC. Preclinical versus clinical drug combination studies. *Leuk Lymphoma.* 2008; 49:2059–2080. [PubMed: 19021049]
- Daniel D, Yang B, Lawrence DA, Totpal K, Balter I, Lee WP, Gogineni A, Cole MJ, Yee SF, Ross S, Ashkenazi A. Cooperation of the proapoptotic receptor agonist rhApo2L/TRAIL with the CD20 antibody rituximab against non-Hodgkin lymphoma xenografts. *Blood.* 2007; 110:4037–4046. [PubMed: 17724141]
- Finn OJ. Cancer immunology. *N Engl J Med.* 2008; 358:2704–2715. [PubMed: 18565863]
- Foran JM, Norton AJ, Micallef IN, Taussig DC, Amess JA, Rohatiner AZ, Lister TA. Loss of CD20 expression following treatment with rituximab (chimaeric monoclonal anti-CD20): a retrospective cohort analysis. *Br J Haematol.* 2001; 114:881–883. [PubMed: 11564080]
- Glennie MJ, French RR, Cragg MS, Taylor RP. Mechanisms of killing by anti-CD20 monoclonal antibodies. *Mol Immunol.* 2007; 44:3823–3837. [PubMed: 17768100]
- Hiraga J, Tomita A, Sugimoto T, Shimada K, Ito M, Nakamura S, Kiyoi H, Kinoshita T, Naoe T. Down-regulation of CD20 expression in B-cell lymphoma cells after treatment with rituximab-containing combination chemotherapies: its prevalence and clinical significance. *Blood.* 2009; 113:4885–4893. [PubMed: 19246561]
- Jaiswal S, Chao MP, Majeti R, Weissman IL. Macrophages as mediators of tumor immunosurveillance. *Trends Immunol.* 31:212–219. [PubMed: 20452821]
- Jaiswal S, Jamieson CH, Pang WW, Park CY, Chao MP, Majeti R, Traver D, van Rooijen N, Weissman IL. CD47 is upregulated on circulating hematopoietic stem cells and leukemia cells to avoid phagocytosis. *Cell.* 2009; 138:271–285. [PubMed: 19632178]
- Katzenberger T, Petzoldt C, Holler S, Mader U, Kalla J, Adam P, Ott MM, Muller-Hermelink HK, Rosenwald A, Ott G. The Ki67 proliferation index is a quantitative indicator of clinical risk in mantle cell lymphoma. *Blood.* 2006; 107:3407. [PubMed: 16597597]

- Kennedy AD, Beum PV, Solga MD, DiLillo DJ, Lindorfer MA, Hess CE, Densmore JJ, Williams ME, Taylor RP. Rituximab infusion promotes rapid complement depletion and acute CD20 loss in chronic lymphocytic leukemia. *J Immunol.* 2004; 172:3280–3288. [PubMed: 14978136]
- Kikuchi Y, Uno S, Kinoshita Y, Yoshimura Y, Iida S, Wakahara Y, Tsuchiya M, Yamada-Okabe H, Fukushima N. Apoptosis inducing bivalent single-chain antibody fragments against CD47 showed antitumor potency for multiple myeloma. *Leuk Res.* 2005; 29:445–450. [PubMed: 15725479]
- Kikuchi Y, Uno S, Yoshimura Y, Otabe K, Iida S, Oheda M, Fukushima N, Tsuchiya M. A bivalent single-chain Fv fragment against CD47 induces apoptosis for leukemic cells. *Biochem Biophys Res Commun.* 2004; 315:912–918. [PubMed: 14985099]
- Kim MJ, Lee JC, Lee JJ, Kim S, Lee SG, Park SW, Sung MW, Heo DS. Association of CD47 with natural killer cell-mediated cytotoxicity of head-and-neck squamous cell carcinoma lines. *Tumour Biol.* 2008; 29:28–34. [PubMed: 18497546]
- Leonard JP, Coleman M, Ketas J, Ashe M, Fiore JM, Furman RR, Niesvizky R, Shore T, Chadburn A, Horne H, et al. Combination antibody therapy with epratuzumab and rituximab in relapsed or refractory non-Hodgkin's lymphoma. *J Clin Oncol.* 2005; 23:5044–5051. [PubMed: 15955901]
- Leonard JP, Friedberg JW, Younes A, Fisher D, Gordon LI, Moore J, Czuczman M, Miller T, Stiff P, Cheson BD, et al. A phase I/II study of galiximab (an anti-CD80 monoclonal antibody) in combination with rituximab for relapsed or refractory, follicular lymphoma. *Ann Oncol.* 2007; 18:1216–1223. [PubMed: 17470451]
- Leonard JP, Schuster SJ, Emmanouilides C, Couture F, Teoh N, Wegener WA, Coleman M, Goldenberg DM. Durable complete responses from therapy with combined epratuzumab and rituximab: final results from an international multicenter, phase 2 study in recurrent, indolent, non-Hodgkin lymphoma. *Cancer.* 2008; 113:2714–2723. [PubMed: 18853418]
- Maddipatla S, Hernandez-Ilizaliturri FJ, Knight J, Czuczman MS. Augmented antitumor activity against B-cell lymphoma by a combination of monoclonal antibodies targeting TRAIL-R1 and CD20. *Clin Cancer Res.* 2007; 13:4556–4564. [PubMed: 17671142]
- Majeti R, Chao MP, Alizadeh AA, Pang WW, Jaiswal S, Gibbs KD Jr, van Rooijen N, Weissman IL. CD47 is an adverse prognostic factor and therapeutic antibody target on human acute myeloid leukemia stem cells. *Cell.* 2009; 138:286–299. [PubMed: 19632179]
- Mateo V, Lagneaux L, Bron D, Biron G, Armant M, Delespesse G, Sarfati M. CD47 ligation induces caspase-independent cell death in chronic lymphocytic leukemia. *Nat Med.* 1999; 5:1277–1284. [PubMed: 10545994]
- Milush JM, Long BR, Snyder-Cappione JE, Cappione AJ 3rd, York VA, Ndhlovu LC, Lanier LL, Michaelsson J, Nixon DF. Functionally distinct subsets of human NK cells and monocyte/DC-like cells identified by coexpression of CD56, CD7, and CD4. *Blood.* 2009; 114:4823–4831. [PubMed: 19805616]
- Nimmerjahn F, Ravetch JV. Antibodies, Fc receptors and cancer. *Curr Opin Immunol.* 2007; 19:239–245. [PubMed: 17291742]
- Oscier DG, Gardiner AC, Mould SJ, Glide S, Davis ZA, Ibbotson RE, Corcoran MM, Chapman RM, Thomas PW, Copplestone JA, et al. Multivariate analysis of prognostic factors in CLL: clinical stage, IGVH gene mutational status, and loss or mutation of the p53 gene are independent prognostic factors. *Blood.* 2002; 100:1177–1184. [PubMed: 12149195]
- Rosenwald A, Wright G, Chan WC, Connors JM, Campo E, Fisher RI, Gascoyne RD, Muller-Hermelink HK, Smeland EB, Giltneane JM, et al. The use of molecular profiling to predict survival after chemotherapy for diffuse large-B-cell lymphoma. *N Engl J Med.* 2002; 346:1937–1947. [PubMed: 12075054]
- Rosenwald A, Wright G, Wiestner A, Chan WC, Connors JM, Campo E, Gascoyne RD, Grogan TM, Muller-Hermelink HK, Smeland EB, et al. The proliferation gene expression signature is a quantitative integrator of oncogenic events that predicts survival in mantle cell lymphoma. *Cancer Cell.* 2003; 3:185–197. [PubMed: 12620412]
- Shipp MA, Ross KN, Tamayo P, Weng AP, Kutok JL, Aguiar RC, Gaasenbeek M, Angelo M, Reich M, Pinkus GS, et al. Diffuse large B-cell lymphoma outcome prediction by gene-expression profiling and supervised machine learning. *Nat Med.* 2002; 8:68–74. [PubMed: 11786909]

- Shultz LD, Lyons BL, Burzenski LM, Gott B, Chen X, Chaleff S, Kotb M, Gillies SD, King M, Mangada J, et al. Human lymphoid and myeloid cell development in NOD/LtSz-scid IL2R gamma null mice engrafted with mobilized human hemopoietic stem cells. *J Immunol.* 2005; 174:6477–6489. [PubMed: 15879151]
- Smith MR. Rituximab (monoclonal anti-CD20 antibody): mechanisms of action and resistance. *Oncogene.* 2003; 22:7359–7368. [PubMed: 14576843]
- Takai T, Li M, Sylvestre D, Clynes R, Ravetch JV. FcR gamma chain deletion results in pleiotropic effector cell defects. *Cell.* 1994; 76:519–529. [PubMed: 8313472]
- Tallarida RJ. An overview of drug combination analysis with isobolograms. *J Pharmacol Exp Ther.* 2006; 319:1–7. [PubMed: 16670349]
- Taylor RP, Lindorfer MA. Immunotherapeutic mechanisms of anti-CD20 monoclonal antibodies. *Curr Opin Immunol.* 2008; 20:444–449. [PubMed: 18585457]
- Uno S, Kinoshita Y, Azuma Y, Tsunenari T, Yoshimura Y, Iida S, Kikuchi Y, Yamada-Okabe H, Fukushima N. Antitumor activity of a monoclonal antibody against CD47 in xenograft models of human leukemia. *Oncol Rep.* 2007; 17:1189–1194. [PubMed: 17390064]

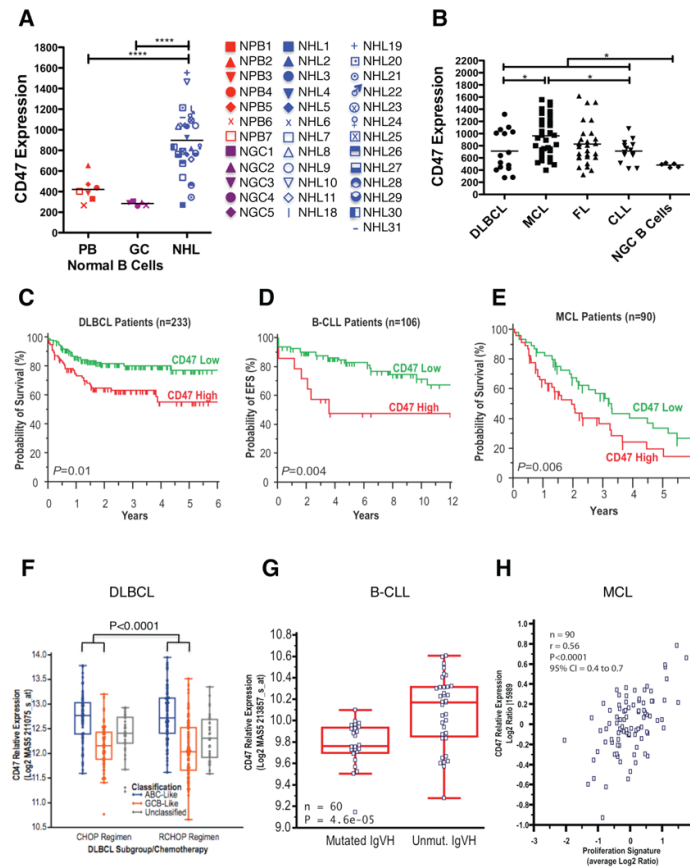


**Figure 1. CD47 Expression is Increased on NHL Cells Compared to Normal B Cells, Confers a Worse Clinical Prognosis, and Correlates with Adverse Molecular Features in Multiple NHL Subtypes**

(A) CD47 expression on normal peripheral blood (PB) B cells (CD19+), normal germinal center (GC) B cells (CD3-CD5-CD20+CD10+CD38+), and NHL B cells (CD19+) was determined by flow cytometry, and mean fluorescence intensity was normalized for cell size. Each point represents a different patient sample: DLBCL=2, CLL=15, MCL=4, FL=6, MZL=2, and pre-B ALL=1 (\*\*\*\* $p < 0.0001$ ). Normalized mean expression (and range) for each population were: normal PB B cells 420.9 (267.3-654.0), normal GC B cells 482.5 (441.1-519.9), and NHL 888.5 (270.1-1553). (B) CD47 expression across NHL subtypes including DLBCL (DL,  $n=15$ ), MCL ( $n=34$ ), FL ( $n=28$ ), and B-CLL ( $n=14$ ) was determined as in A. Normalized mean expression (and range) for each population were: DL 725.7 (261.2 – 1344), MCL 1055 (444.2-2196), FL 825.1 (283.6-1546), CLL 713.6 (432.8-1086), (\* $p < 0.05$ ). (B to D) Prognostic influence of *CD47* mRNA expression is shown on overall (C and E) and event-free (D) survival of patients with DLBCL, B-CLL, and MCL. For DLBCL and CLL, stratification into low and high CD47 expression groups was based on an optimal threshold determined by microarray analysis; this cut point was internally validated for both DLBCL and CLL, and also externally validated in an independent DLBCL cohort. For MCL, stratification relative to the median was employed as an optimal cut point could not be defined. Significance measures are based on log-likelihood estimates of the p-value, when treating *CD47* expression as a continuous variable, with corresponding dichotomous indices also provided in Table S1. (F to H) *CD47* mRNA expression is shown in relation to cell-of-origin classification for DLBCL (F), immunoglobulin heavy chain mutation status (IgVH) for CLL (G), and proliferation index for MCL (H). Analyses for C-H employed publicly available datasets for NHL patients (Table S1). NGC=normal germinal center,

ABC=activated B cell-like, GCB=germinal center B cell-like. See also Figure S1 and Table S1.



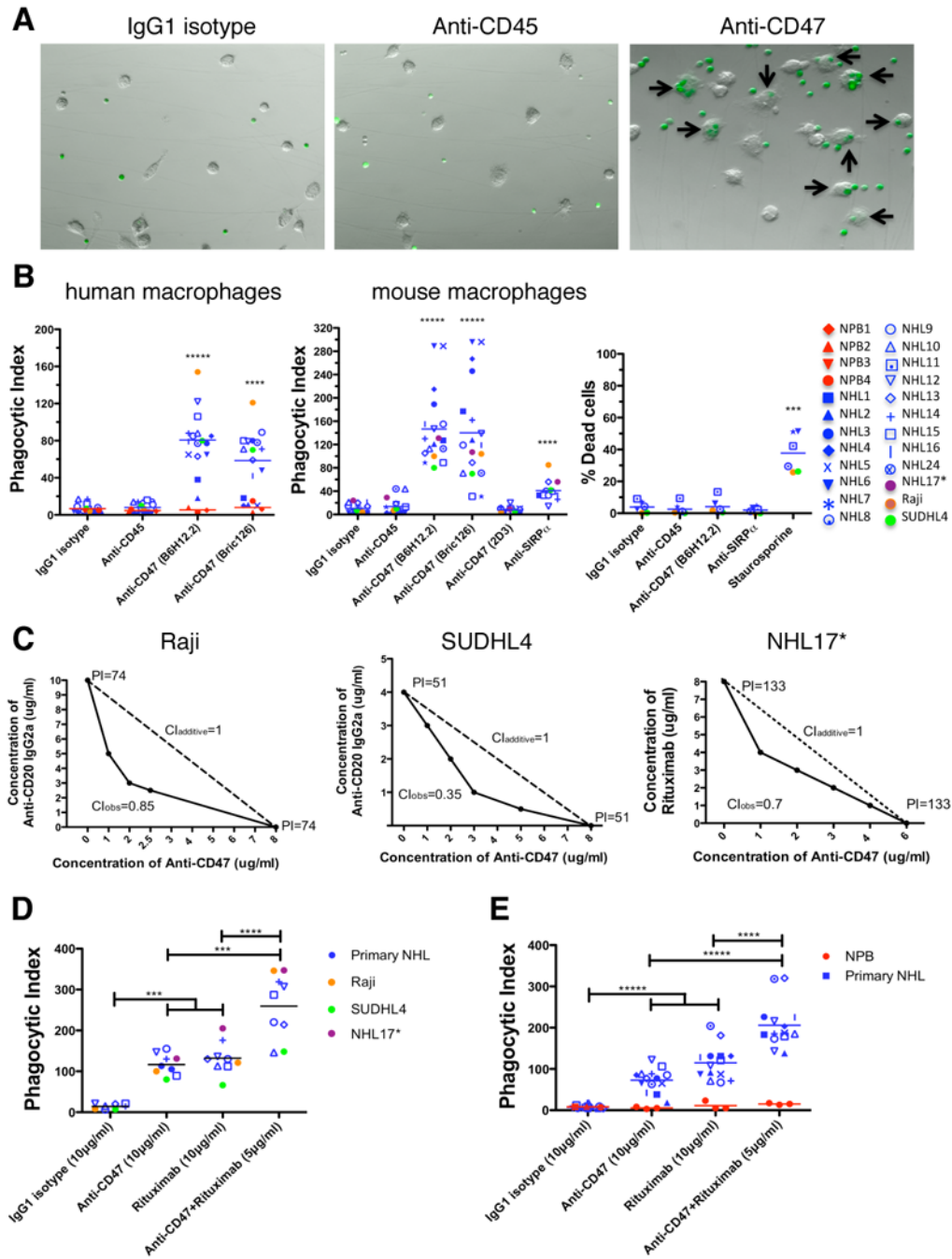


**Figure 2. Blocking Antibodies Against CD47 Enable Phagocytosis of NHL Cells by Macrophages and Synergize with Rituximab *in Vitro***

(A) CFSE-labeled NHL cells were incubated with human macrophages and the indicated antibodies and examined by immunofluorescence microscopy to detect phagocytosis (arrows). Photomicrographs from a representative NHL sample are shown. (B) Phagocytic indices of primary human NHL cells (blue), normal peripheral blood (NPB) cells (red), and NHL cell lines (purple, orange, and green) were determined using human (left) and mouse (middle) macrophages. Antibody-induced apoptosis (right panel) was tested by incubating NHL cells with the indicated antibodies or staurosporine without macrophages, and assessing the percentage of apoptotic and dead cells (% annexin V and/or PI positive). (C)

Synergistic phagocytosis by anti-CD47 antibody (B6H12.2) and anti-CD20 mAbs was examined by isobologram analysis and determination of combination indices (CI).  $CI_{obs}$  indicates observed results, and the dashed line indicates the expected results if antibodies were additive. (D,E) Synergy between anti-CD47 antibody and rituximab in the phagocytosis of NHL and NPB cells was assessed by determining the phagocytic index when incubated with a combination of both antibodies compared to either antibody alone at twice the dose, with either mouse (D) or human (E) macrophages. NHL17\*: cell line derived from primary sample NHL17. \*\*\* $p < 0.001$ , \*\*\*\* $p < 0.0001$ , \*\*\*\*\* $p < 0.00001$ . Figure 2B p-values represent comparison against IgG1 isotype control antibody. See also Figure S2.

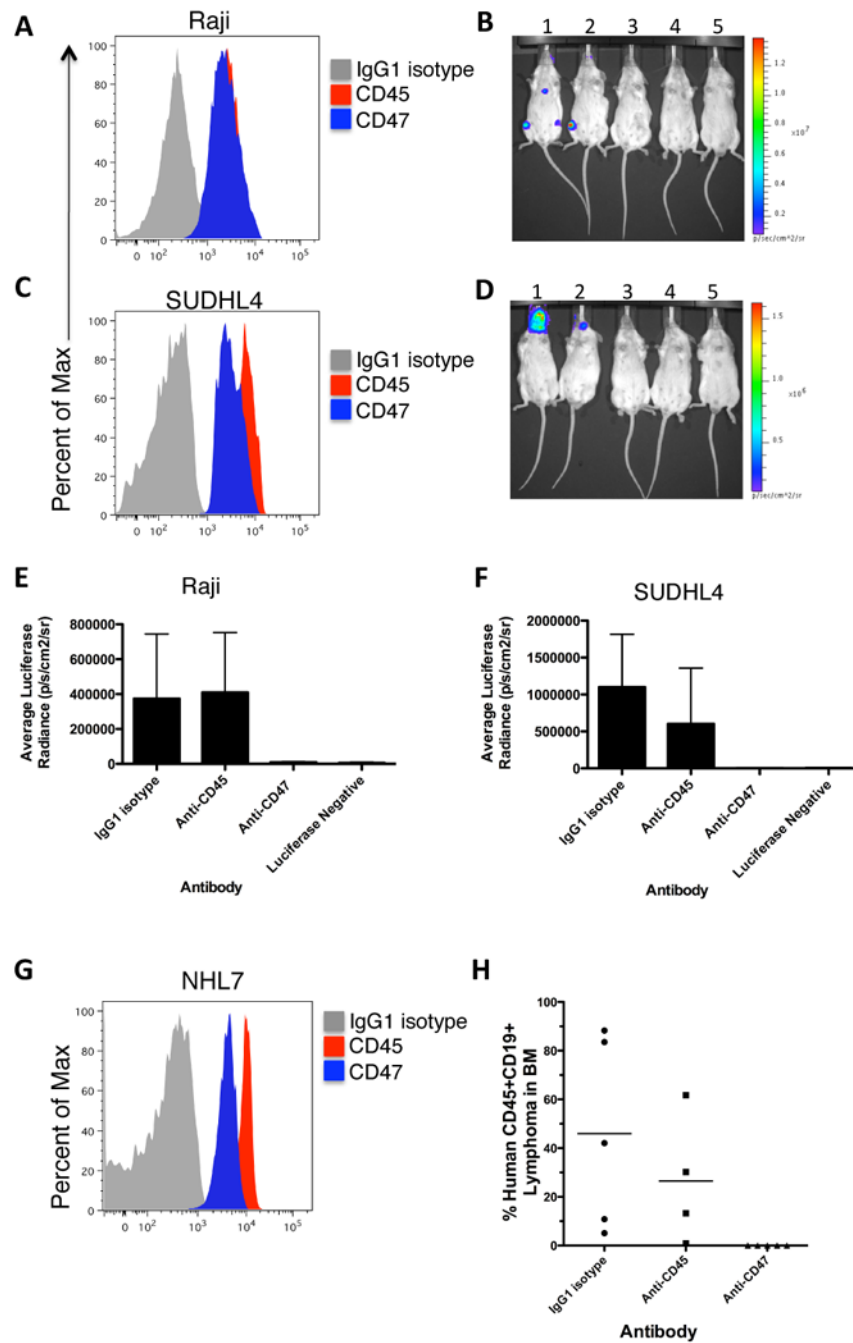


### Figure 3. Ex Vivo Coating of NHL Cells with an Anti-CD47 Antibody Inhibits Tumor Engraftment

(A-F) Luciferase-expressing Raji (A) and SUDHL4 (C) cells were assessed for *ex vivo* antibody coating by flow cytometry. SCID mice transplanted with Raji (B) and SUDHL4 (D) were subject to bioluminescent imaging (1-IgG1 isotype control, 2-anti-CD45, 3 and 4-anti-CD47, 5-luciferase negative control). Bioluminescence for Raji (E) and SUDHL4 (F) engrafted mice was quantified (n=3 per antibody condition). No tumor engraftment was observed in mice transplanted with anti-CD47-coated cells compared to IgG-coated cells ( $p < 0.05$ ) for both Raji and SUDHL4, as assessed by bioluminescent imaging. Data are represented as mean  $\pm$  SD. (G) Bulk lymphoma cells from a human NHL patient were

assessed for *ex vivo* antibody coating by flow cytometry. (H) Compared to IgG1 isotype control, anti-CD47 antibody pre-treatment inhibited engraftment of NHL cells ( $p < 0.0001$ ) while anti-CD45 coated cells engrafted similarly to controls ( $p = 0.54$ ). All p-values were determined using Fisher's exact test. See also Figure S3.

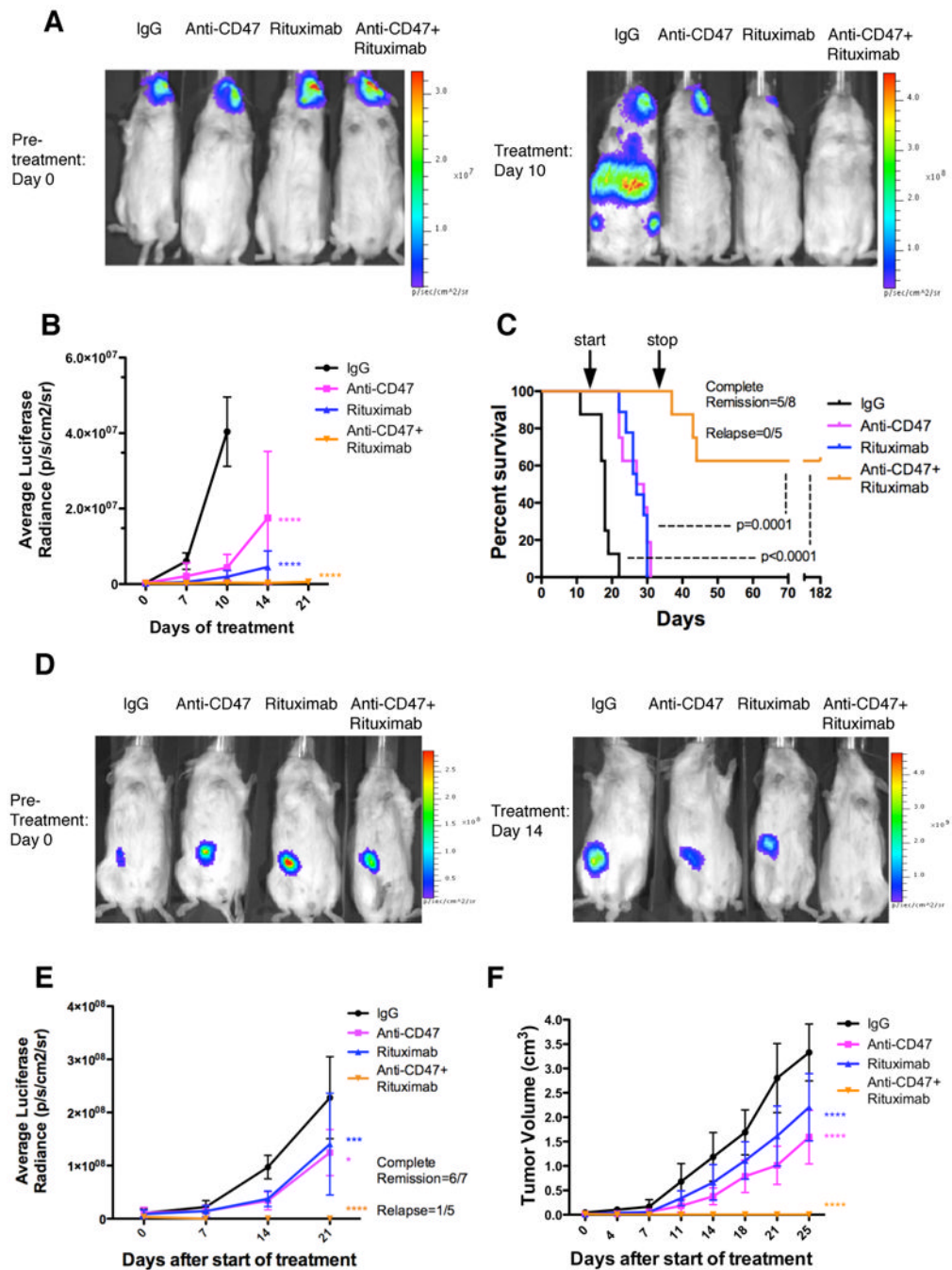


**Figure 4. Combination Therapy with anti-CD47 Antibody and Rituximab Eliminates Lymphoma in both Disseminated and Localized Human NHL Xenotransplant Mouse Models** (A) NSG mice transplanted intravenously with luciferase-expressing Raji cells were treated with the indicated antibodies (n=8 per treatment group). Luciferase imaging of representative mice from pre- and 10 days post-treatment are shown (A) and averaged for all mice in each treatment group (B). (C) Kaplan-Meier survival analysis was performed (Table S2). p-values compare IgG control to combination antibody treatment or anti-CD47 antibody/rituximab single antibody to combination. Arrows indicate start (day 14) and stop (day 35) of treatment. (D) Luciferase-expressing Raji cells were transplanted subcutaneously in the flank of NSG mice. When palpable tumors (~0.1cm<sup>3</sup>) formed, treatment began with

the indicated antibodies. Luciferase imaging of representative mice from each treatment group is shown before (day 0) and during (day 14) treatment. (E) Quantified bioluminescence was determined and averaged for all mice in each treatment group (n=7). (F) Tumor volume was measured with average volume shown. p-values were derived from a two-way ANOVA and compared to IgG treatment. \*p<0.05, \*\*\*p<0.001, \*\*\*\*p<0.0001. Complete remission was defined as the number of mice with no evidence of tumor at the indicated date. Relapse was defined as the number of mice achieving a complete remission that later developed recurrence of tumor growth. For panel E, one mouse that achieved a complete remission died of non-tumor related causes. Data presented in B, E, and F are mean values +/- SD. See also Figure S4 and Table S2.

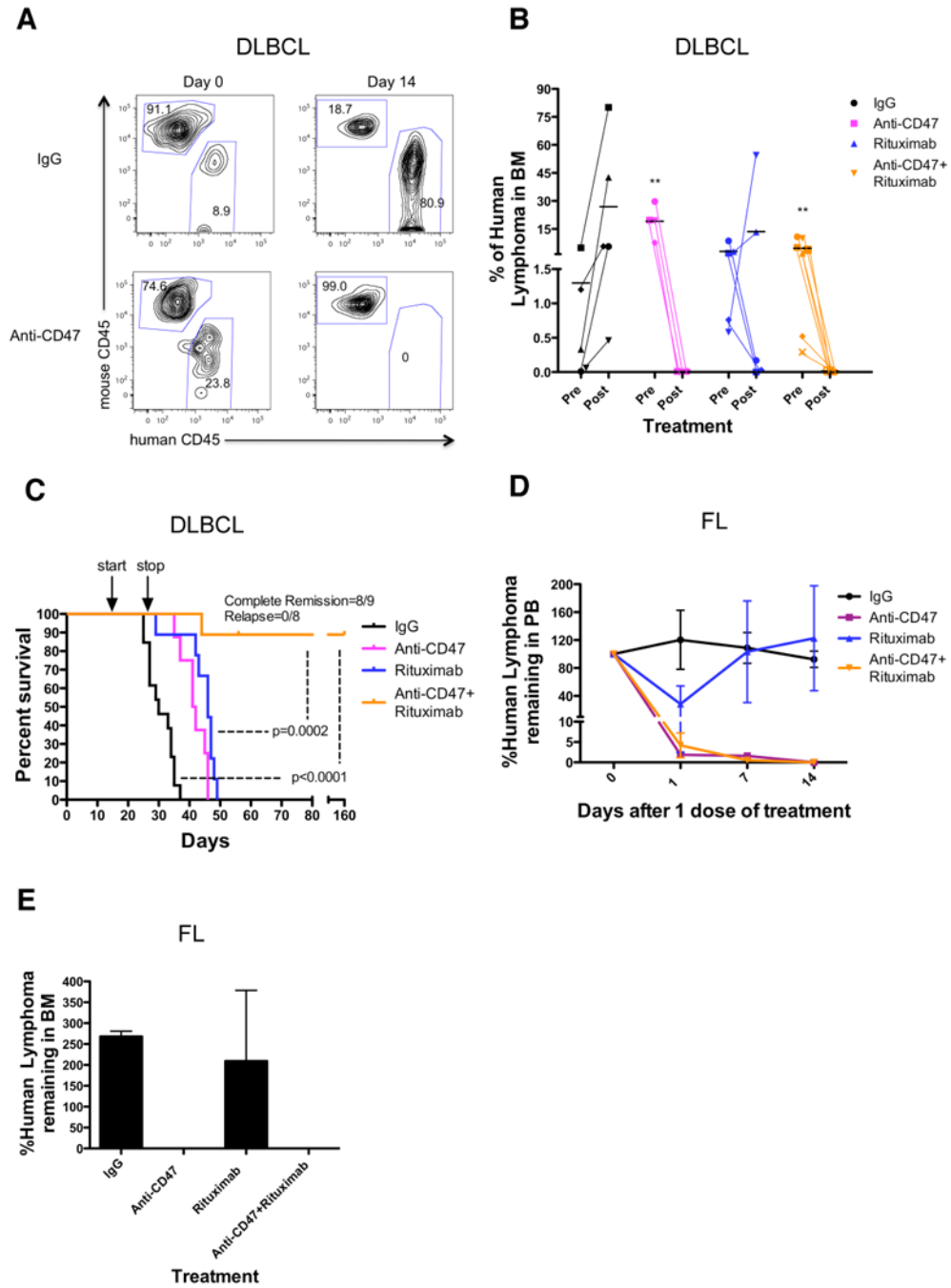


**Figure 5. Combination Therapy with Anti-CD47 Antibody and Rituximab Eliminates Lymphoma in Primary Human NHL Xenotransplant Mouse Models**

(A,B) Sublethally-irradiated NSG mice were transplanted intravenously with cells from a primary DLBCL patient (NHL7) and treated with the indicated antibodies. Flow cytometry of human lymphoma engraftment in the bone marrow of two representative mice is shown pre- and 14 days post-antibody treatment in (A). Data from all mice is included in (B).

\*\* $p<0.01$ , comparing pre- and post-treatment values for each respective antibody treatment. (C) Kaplan-Meier survival analysis (Table S3) of DLBCL-engrafted mice from each antibody treatment cohort is shown ( $n\geq 10$  per antibody group), with p-values calculated comparing control IgG to combination antibody treatment or anti-CD47 antibody/rituximab

single antibody to combination treatment. Arrows indicate start (day 14) and stop (day 28) of treatment. (D-E) Mice engrafted intravenously with a primary FL patient sample (NHL31) were treated with a single dose of the indicated antibodies. Compared to IgG control and rituximab, anti-CD47 antibody alone or in combination with rituximab eliminated tumor burden in the peripheral blood ( $p=0.04$ , 2-way ANOVA), and bone marrow ( $p<0.001$ , t-test). (E) Lymphoma engraftment in the bone marrow was determined 14 days post-treatment. Each antibody treatment group consisted of 3 mice. For mice reported in panels D and E, human lymphoma chimerism was between 5-25% in the peripheral blood and bone marrow. See also Figure S5 and Table S3.



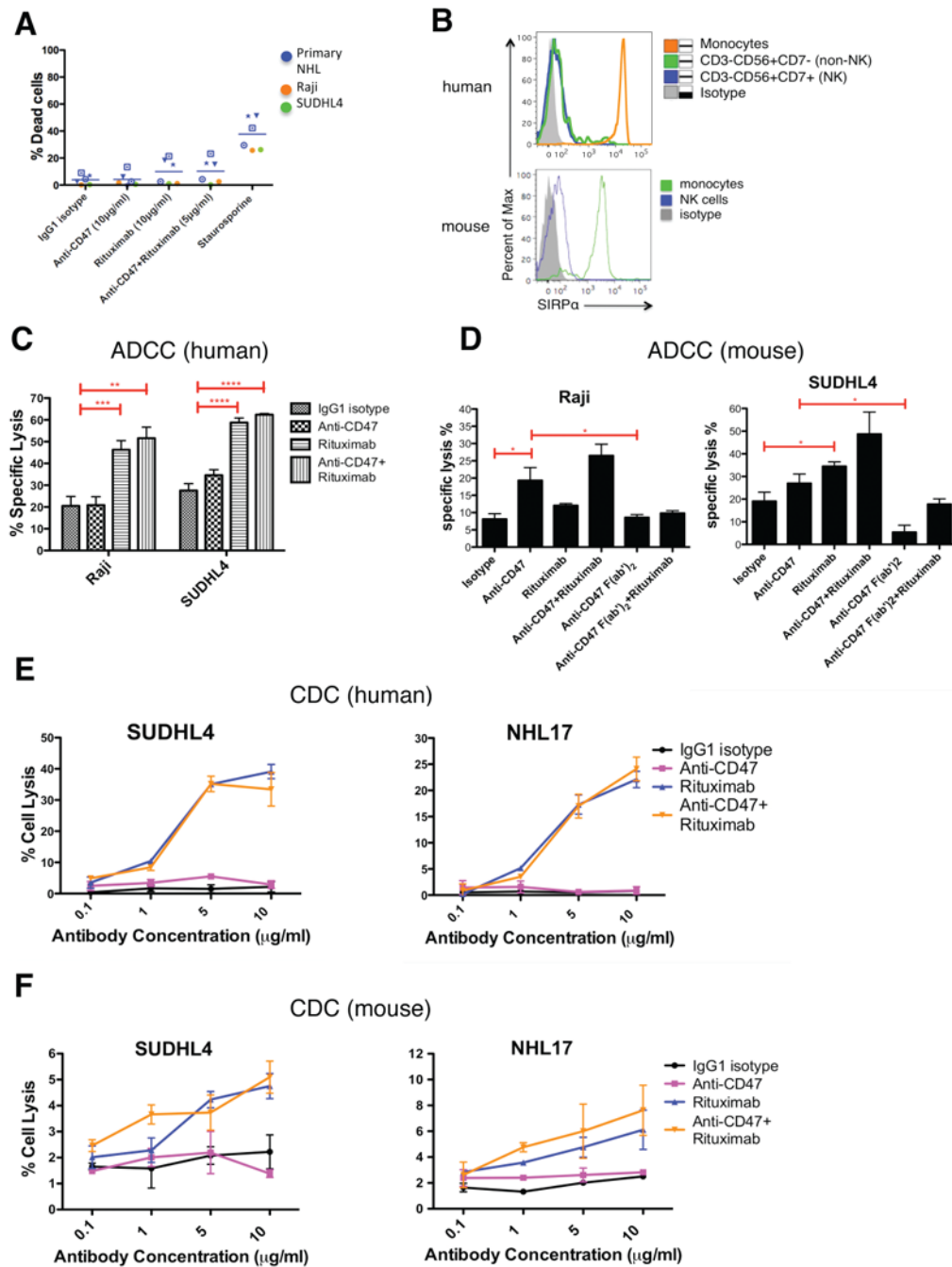


**Figure 6. Synergy Between Anti-CD47 Antibody and Rituximab Does Not Occur Through NK Cells or Complement**

(A) NHL cells were incubated with the indicated soluble antibodies for 2 hours and the percentage of dead cells was calculated (% Annexin V+ and/or 7-AAD+). No statistically significant difference in % dead cells was observed with the combination of anti-CD47 antibody and rituximab compared to either anti-CD47 antibody alone ( $p=0.24$ ) or rituximab alone ( $p=0.95$ ). (B) SIRP $\alpha$  expression is shown for both human and mouse NK cells as determined by flow cytometry. (C,D) Chromium release assays measuring ADCC were performed in triplicate with human (C) and mouse (D) at an effector:target ratio of 17.5:1 and percent specific lysis is reported. Antibodies were incubated at 10 $\mu$ g/ml except anti-

CD47 full length or F(ab')<sub>2</sub> antibody+rituximab (5μg/ml). (E) CDC assay with human complement was performed in duplicate. Compared to IgG1 isotype control, anti-CD47 antibody did not enable CDC ( $p>0.2$ ), while rituximab did ( $p<0.001$ ) by 2-way ANOVA for both SUDHL4 and NHL17\*. Combination treatment with anti-CD47 antibody and rituximab did not enable greater levels of CDC compared to rituximab ( $p=0.78$ ). (F) CDC assay with mouse complement was performed in duplicate. Compared to IgG1 isotype control, anti-CD47 antibody did not enable CDC ( $p>0.25$ ) while rituximab did ( $p=0.03$ ,  $p=0.08$ , respectively) for both SUDHL4 and NHL17\*. No difference in CDC between CD47 antibody+rituximab and rituximab alone was observed ( $p>0.13$ ) for both SUDHL4 and NHL17\*. \* $p<0.05$ , \*\* $p<0.01$ , \*\*\* $p<0.001$ , \*\*\*\* $p<0.0001$ . NHL17\*=Primary NHL17 cells expanded in culture. See also Figure S6.

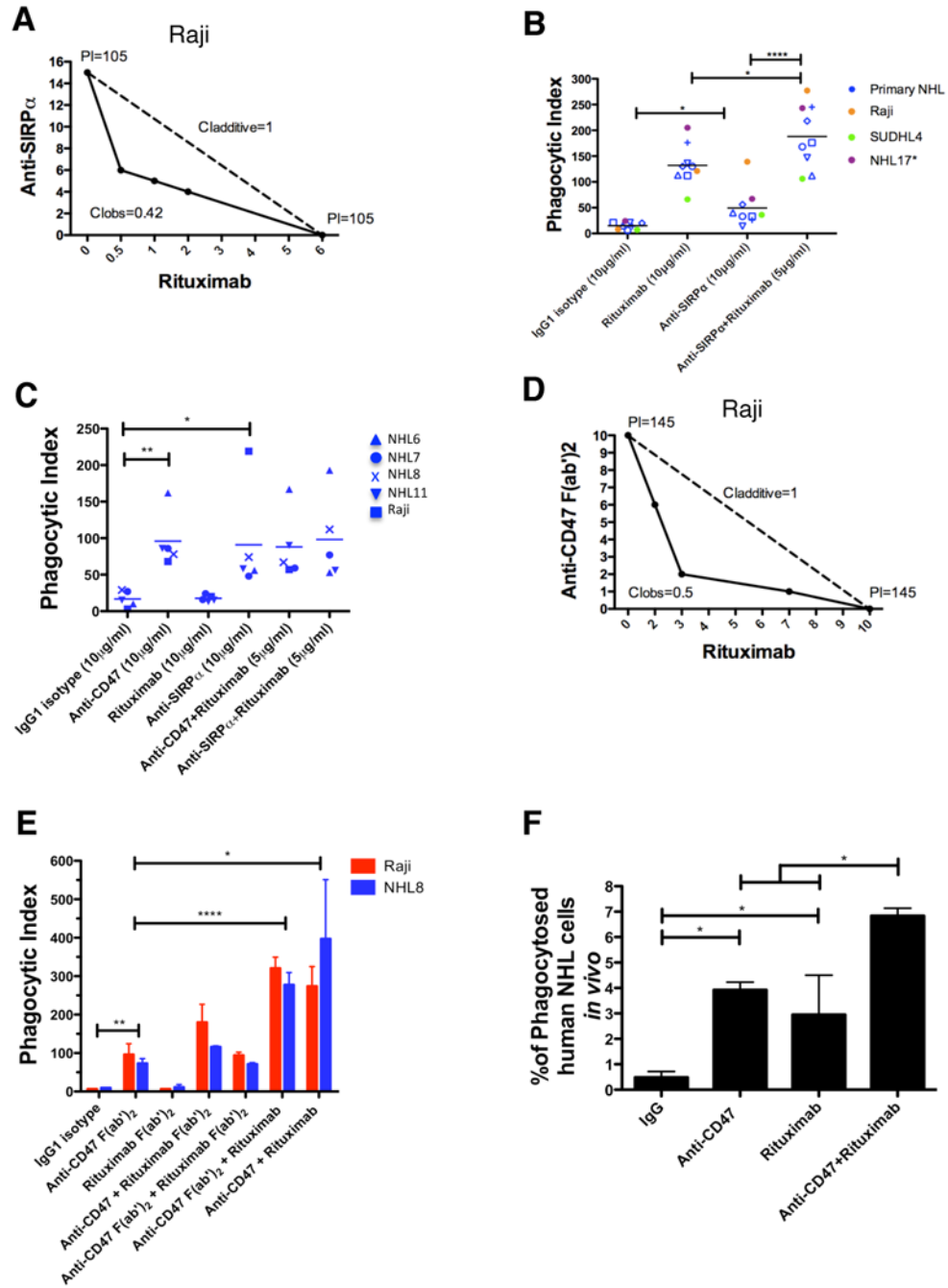


**Figure 7. Anti-CD47 Antibody Synergizes with Rituximab Through FcR-Independent and FcR-Dependent Mechanisms**

(A) Isobologram analysis of phagocytosis induced by anti-SIRP $\alpha$  antibody and rituximab is shown for Raji cells and mouse macrophages. (B,C) NHL cells were incubated *in vitro* with the indicated antibodies in the presence of wild type (B) or Fc $\gamma$ R $^{-/-}$  (C) mouse macrophages, and the phagocytic index was determined. (D) Isobologram analysis of phagocytosis induced by anti-CD47 F(ab) $_2$  antibody and rituximab is shown for Raji cells and mouse macrophages. (E) NHL cells were incubated with wild type mouse macrophages in the presence of the indicated full length or F(ab) $_2$  antibodies (single antibodies at 10 $\mu$ g/ml, combination antibodies at 5 $\mu$ g/ml each) and the phagocytic index was determined. (F) The

level of *in vivo* phagocytosis measured as the percentage of mouse macrophages containing phagocytosed GFP+ Raji cells (hCD45-GFP+F4/80+) was determined by flow cytometry of livers from mice engrafted with GFP+ Raji cells and then treated with the indicated antibodies (see methods), with each treatment group performed in duplicate. Compared to IgG control, anti-CD47 antibody and rituximab enabled increased levels of phagocytosis. Compared to anti-CD47 antibody alone, combination anti-CD47 antibody and rituximab enabled higher levels of phagocytosis. \* $p < 0.05$ , \*\* $p < 0.01$ , \*\*\*\* $p < 0.0001$ . See also Figure S7.